Organic & Biomolecular Chemistry

ROYAL SOCIETY OF CHEMISTRY

COMMUNICATION

View Article Online
View Journal | View Issue

Cite this: *Org. Biomol. Chem.*, 2021, **19**, 574

Received 2nd October 2020,
Accepted 21st December 2020

DOI: 10.1039/d0ob02016h

rsc.li/obc

Silicon-rhodamine isothiocyanate for fluorescent labelling†

Veselin Nasufović,[a] Patrick Then,[b] Fabian Dröge,[c] Michael Duong,[a] Christoph Kaether,[d] Benjamin Dietzek,[b,c] Rainer Heintzmann[b,c] and Hans-Dieter Arndt*[a]

An efficient synthesis for silicon-rhodamines was developed, enabling the preparation and evaluation of silicon-rhodamine isothiocyanate (SITC) as a novel tool for facile fluorescent labeling. Ease of use in conjugation to amino groups, high stability and excellent photophysical properties are demonstrated. SITC-actin was found to be neutral to F-actin polymerization induction and well suited for high resolution fluorescence microscopy.

With its first synthesis by Adolf von Baeyer in 1871, fluorescein was applied as a staining reagent.[1] By employing amino phenols instead of resorcinols, rhodamines were prepared.[2] Fluorescein-isothiocyanate (FITC, **1**, Fig. 1) was subsequently developed for specific labelling, combining ease of synthesis with ease of use.[3–5] The spectral properties of FITC conjugates mimic fluoreceine.[5] FITC reacts with a variety of nucleophiles, but in water it is fairly selective for free amino groups in peptides and proteins.[6] FITC has been the first fluorescent label that was successfully conjugated to antibodies[3–5] and was used extensively.[7–12] It keeps to be widely applied in immunofluorescence,[13,14] labelling of biomolecules,[15] surfaces, or in FRET couples.[16] Unfortunately, the common synthesis of FITC is not regioselective, but forms regioisomers (Fig. 1).

More recently, isoelectronic exchange of oxygen for other heteroatoms has provided fluorophores with improved properties such as high absorptivity, red-shifted absorption and emission, enhanced photostability, and cell permeability.[17] *In cellulo* and *in vivo* experiments were realized,[18–22] as well as FRET experiments.[23] Among them, silicon-rhodamine (SiR) is a particularly bright fluorophore with high extinction coefficient and quantum yield.[24] Its favourable "*spiro*" to "*open*" state equilibrium enhances cell permeability and can make probes fluorogenic, rendering SiR a useful tool in super-resolution microscopy.[17,24–26] Although SiRs have been proven to be very useful fluorescent labels, syntheses of SiR-COOH (**2**) and its variants are challenging and are hampered by low yields. Furthermore, additional approaches for introduction of groups suitable for (bio)conjugation are desirable. Herein, we report an improved, scalable protocol for silicon-rhodamine preparation, as well as a regioselective synthesis and first applications of the novel SiR isothiocyanate (SITC, **3**) that suggests diversified analogs to be easily accessible.

Initially, SiRs have been synthesized from 10-*sila*-anthrones by nucleophilic addition of metallated terephthalic acid fragment surrogates.[27,28] Condensation chemistry similar to fluorescein and rhodamine synthesis proved to be low yielding.[29] Enhanced yields were reported by inverting polarity in using

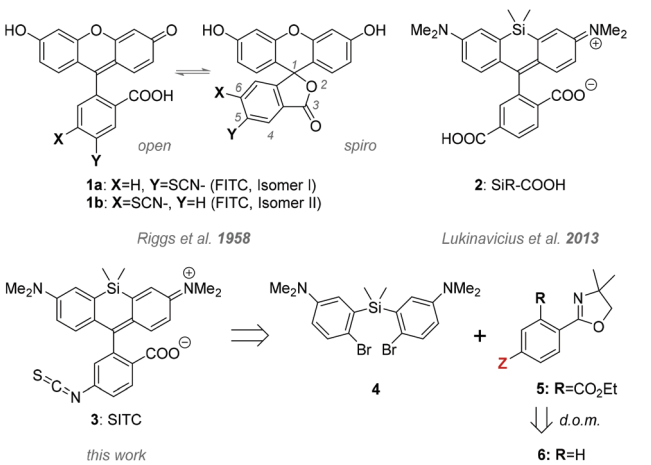

Fig. 1 Fluorescein isothiocyanates, silicon-rhodamine, and SITC: structures and synthesis planning. **5a**, **6a**: Z = 4,4-dimethyloxazolin-2-yl; **5b**, **6b**: Z = OTIPS.

[a]*Friedrich-Schiller-University, Institute of Organic Chemistry and Macromolecular Chemistry, Humboldtstr. 10, 07743 Jena, Germany. E-mail: hd.arndt@uni-jena.de*
[b]*Leibniz-Institut of Photonic Technologies (Leibniz-IPHT), Albert-Einstein-Str. 9, 07745 Jena, Germany*
[c]*Friedrich-Schiller-University, Institute of Physical Chemistry, Helmholtzweg 4, 07743 Jena, Germany*
[d]*Leibniz-Institute on Aging – Fritz Lipmann Institute (FLI), Beutenbergstr. 11, 07745 Jena, Germany*

†Electronic supplementary information (ESI) available. See DOI: 10.1039/d0ob02016h

dimetallated diarylsilanes electrophiles.[30,31] In order to access the target compounds even more effectively, we envisioned to desymmetrize the *para*-substituted aryl oxazolines **6** by directed *ortho* metalation and acylation (→**5**), which could directly lead to SiR derivatives from dibromide **4**.[31] Indeed, cheap terephthalaldehyde (**7**) smoothly underwent double *N*,*O*-acetalization followed by oxidation with NBS in one pot, to give bisoxazoline **6** in 91% yield (Scheme 1).[32] *ortho*-Metalation by employing the TMPMgCl·LiCl reagent[33,34] followed by acylation with benign diethyl pyrocarbonate provided ester **5a** in very good yield. The 1,5-dilithium reagent derived by double Li–Br exchange of dibromide **4** smoothly added to ester **5a**. Acidic dehydration and hydrolysis of the oxazoline protecting groups gave SiR-COOH (**2**). Importantly, in contrast to other reported protocols, this procedure was robustly reproduced by us on the >1 g scale (50% yield from **7**, see ESI, Fig. S7†).

Diacid **2** was then regioselectively converted to Boc-protected aniline **8** by treatment with stoichiometric DPPA and *t*BuOH (63% yield). This regioselective transformation is likely enabled by a spiro-lactone intermediate present at basic conditions (cmp. Fig. 1). Acid-mediated deprotection gave aniline **9** (79% yield) that was transformed to isothiocyanate **3** (SITC) by using thiophosgene (72% yield). This sequence (Scheme 1, e–g) could be executed without chromatography of intermediates **8** and **9** in an enhanced overall yield (64% from **2**). Unfortunately, a more direct introduction of amino groups failed (see ESI, Schemes S2 and 3†). However, intermediate **8** was alternatively accessed by preparing the phenol **10** from TIPS-protected *para*-hydroxybenzaldehyde *via* oxazoline **6e**, similar to **2** (4 steps, see ESI, Scheme S4†). Triflation and Buchwald–Hartwig-type carbamoylation then gave carbamate **8** by avoiding hazardous acyl azide intermediates. Either route (azide-free or -containing) gave SITC as a single regioisomer.

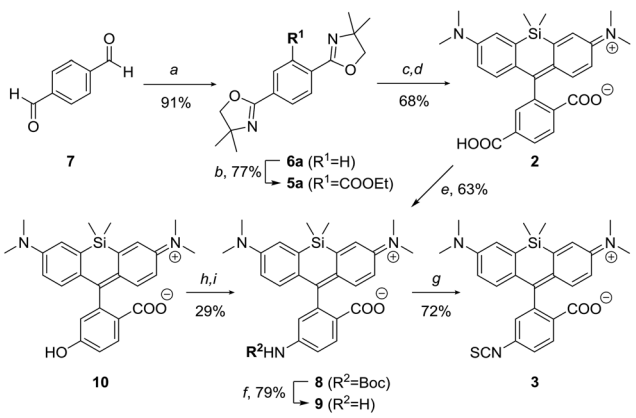

Scheme 1 SiR-COOH and SITC synthesis. Reagents and conditions: (a) 2-Amino-isobutanol, mol. sieves 4 Å, CH_2Cl_2, 25 °C, 16 h, then: NBS, 3 h, 91%; (b) TMPMgCl·LiCl, 25 °C, 4 h, then: DEPC, −15 °C to 25 °C, 3 h, 77%; (c) **4**, *t*-BuLi, −78 °C, 30 min then: **6**, to 25 °C, 16 h; (d) 6 M HCl, 36 h, 68% (2 steps); (e) DPPA, DIPEA, toluene, *t*-BuOH, 90 °C, 16 h, 63%; (f) TFA/CH_2Cl_2 (3 : 7), 0 °C, 2 h, 79%; (g) $Cl_2C{=}S$, NEt_3, CH_2Cl_2, 25 °C, 1 h, 72%; (h) Tf_2O, NEt_3, CH_2Cl_2, 0 °C, 1 h; (i) Pd(dppf)Cl_2, Xantphos, Cs_2CO_3, $H_2NCOOtBu$, 1,4-dioxane, 100 °C, 18 h, 29% (2 steps).

The reactivity of SITC was briefly investigated. SITC is stable on storage and reacts cleanly with amine nucleophiles in organic solvents (DMF, CH_2Cl_2, THF) to give thiocarbamates in good yield (Scheme S5, Fig. S3†). SITC is surprisingly stable in aqueous medium (pH 9 carbonate buffer, 24 h, 25 °C or 37 °C, Fig. S1 and 2†), and reacts with amines in water rather slowly, even at 37 °C (Fig. S2†). Despite slow conversion, selective conjugation with primary amines could be observed (Fig. S4†). Importantly, SITC was found to be stable to thiols, DMAP, and TCEP in aqueous buffer (Fig. S5†).

Spectral properties of SITC conjugates and the novel SiR derivatives were investigated next. For this purpose, SITC was conjugated to methyl ε-aminocaproate (SITC-Ahx, Scheme S5†) and compared to SiRs **2**, **8**, **9**, and **10** (Fig. 2, Table 1). Absorbance and emission were found maximal around pH 3 (Fig. 2c), where a xanthene monocation likely predominates in its open form (ESI, Scheme S1†). Wavelength maxima of absorption and emission lie in the deeply red region (around 645 and 665 nm, respectively), only moderately influenced by

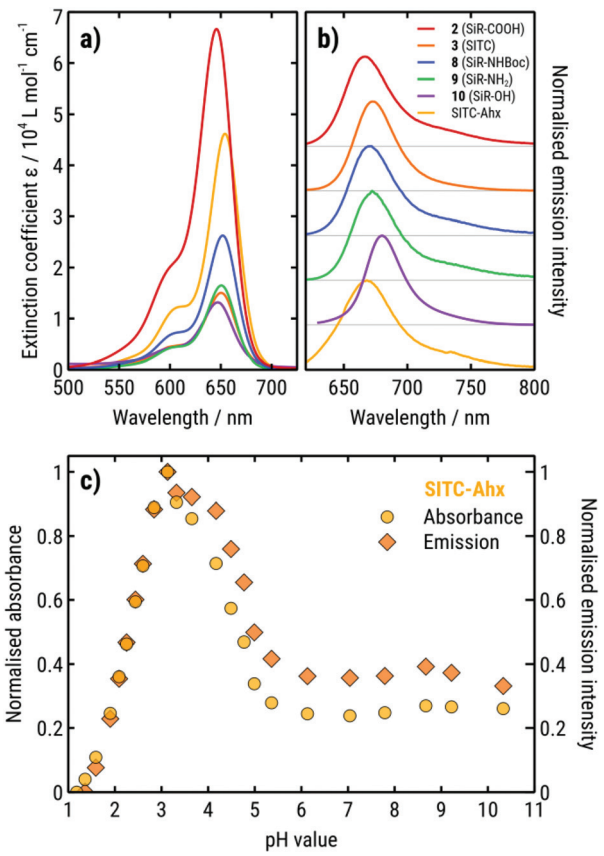

Fig. 2 Normalized UV-Vis absorption (a) and fluorescence emission spectra (b) of SiR compounds in aqueous phosphate-citrate buffer with 20 vol% DMSO at pH 3.14, aqueous TBS buffer with 20 vol% DMSO at pH 7.4 (SiR-COOH, **2**) or aqueous solution with 1.7 vol% DMSO adjusted to pH 3 (SiR-OH, **10**), using a concentration range from 0.1 μM to 100 μM; (c) pH dependent UV-Vis absorption and fluorescence emission maxima of the SITC-Ahx conjugate in aqueous solutions with pH ranging from 1.36 to pH 10.33 supplemented with 10 vol% DMSO (for spectra see Fig. S6 in the ESI†).

Table 1 Spectral properties of synthesized silicon–rhodamines

	2	8	9	3	10	SITC-Ahx
$\lambda_{abs\ (max)/nm}$	645	652	650	651	645	654
$\lambda_{em\ (max)/nm}$	666	669	672	673	665	670
$\varepsilon/10^3$ L mol^{-1} cm^{-1}	67	26	16	15	13	46
Φ^{em}	0.41	0.33	0.04	0.31	n.d.	0.39
pK_a	n.d.	2.4, 4.1	2.7, 4.4	n.d.	n.d.	2.3, 4.4

the aryl substituent, with a small bathochromic shift found for the SITC conjugate. With exception of (basic) aniline **9** and phenol **10**, absorption and quantum yield of emission were high (ε = 2.6–6.7 × 10^4 L mol^{-1} cm^{-1}; ϕ^{em} = 0.33–0.41; Table 1).

In very acidic medium (pH < 2) the absorbance of SITC drops, suggesting the formation of a deconjugated, non-fluorescent spiro-dication (ESI, Scheme S1, Fig. S6†). By contrast, considerable absorption and emission is still found when the medium gets less acidic (pH > 4). Here, the zwitterionic neutral form predominates, equilibrating between fluorescent open and non-fluorescent closed states, influenced by the local environment. This property is believed to facilitate cell permeability and fluorogenicity of SiR conjugates in cell microscopy,[26] and is retained for SITC. Notably, spectral properties of SITC conjugates are constant at biologically relevant pH (5–11), rendering them useful for a wide range of applications in biochemistry and biology.

Conjugation of SiR-COOH (**2**) to an optimized natural product analog of jasplakinolide creates a cell permeable agent for staining the F-actin cytoskeleton.[26] This SiR-Actin reagent **11** (Fig. 3) has become a far-red emissive phalloidin alternative that can be equally used in fixed or living cells. For a detailed comparison, the conjugate **12** (Fig. 3) was synthesized (2 steps, see ESI, Scheme S6†) and investigated in cell microscopy. Generally, SITC-Actin (**12**) exhibited good fluorescence properties which were qualitatively similar to SiR-Actin in terms of brightness and photostability (Fig. S10†). Staining of fixed, but non-embedded HeLa cells along the protocols developed for SiR-actin uncovered highly selective staining of actin filaments (Fig. 4a), comparable to SiR-Actin (Fig. 4c), using a standard Zeiss Elyra microscope. For enhanced resolution and contrast, the SIM-mode could be used in which both dyes showed comparable properties (Fig. 4b and d).

Despite their similarity, SITC-Actin and SiR-Actin display somewhat distinct features. In practice, SITC-Actin showed better staining when lower concentrations were used (150 nM)

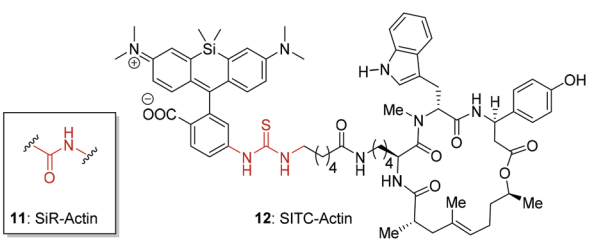

Fig. 3 SITC-actin thiourea conjugate **12** of an optimized jasplakinolide analog.

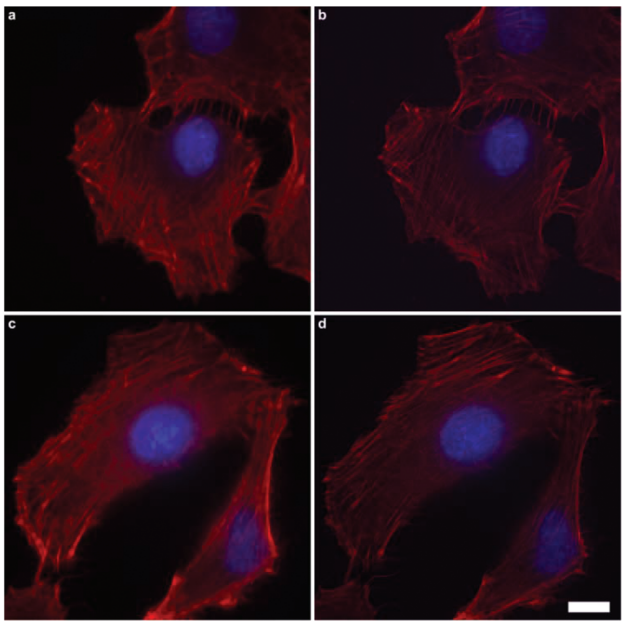

Fig. 4 Fluorescence microscopy images of fixed HeLa-cells. Cells were stained with SITC-actin (a and b) or SiR-Actin (c and d), imaged in the red channel, and with DAPI, imaged in the blue channel. a + c: widefield, b + d: SIM images of the same area; c(probe) = 300 nM, 3 h; see ESI† for experimental conditions. Scalebar is 10 µm.

over longer time (6–12 h, Fig. S9†), whereas SiR-Actin showed good staining at higher concentration with shorter exposure (1 µM for 1–2 h). Interestingly, at elevated excitation intensity, SITC-Actin displayed spontaneous blinking in PBS buffer (Fig. S11†). While this property may reduce the fluorescence signal in widefield fluorescence microscopy imaging, it could potentially be exploited for single molecule localization microscopy (SMLM) techniques such as dSTORM.[35]

SITC-Actin is a fluorogenic compound (3.1-fold increase of fluorescence upon binding to F-actin), slightly less so than SiR-Actin (5-fold increase), but with similar binding kinetics (Fig. S8†). When tested in actin depolymerization assays (high salt), both SiR-Actin and SITC-Actin retarded F-actin dissolution, similarly to jasplakinolide (Fig. S9a†). When monitoring G-actin polymerization at low salt conditions, jasplakinolide strongly promoted this process, as expected. By contrast, SITC-Actin performed completely neutral, whereas SiR-Actin even slightly decelerated F-actin assembly (Fig. S9b and c†). These data indicate that by introducing different labels, actin tool compound properties and toxicity can be engineered, likely by influencing individual compound folding and aggregation or by modulating G-actin binding, as suggested previously.[36]

In terms of live cell application, both SITC- and SiR-Actin feature no detectable toxicity at the concentrations used for live imaging (≤1 µM), in contrast to the highly toxic jasplakinolide (Fig. S12†). This beneficial feature, which may correlate with the much reduced propensity for F-actin polymerization induction by SIR- and SITC-Actin, renders these tool compounds essentially non-toxic in the low-µM range and hence well suited for undistorted live-cell imaging.[26]

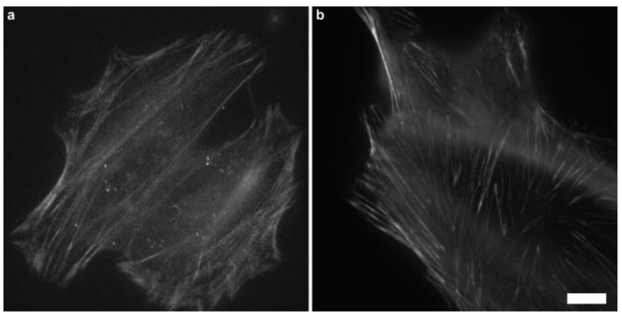

Fig. 5 Fluorescence microscopy images of live HeLa cells stained with SITC-actin (a) and SiR-Actin (b). Cells were incubated in medium containing 1 μM dye for one hour, with cells washed prior to imaging. Scale bar is 10 μm.

SITC-Actin was indeed found to be cell permeable, but live cell imaging needed slight adjustments of conditions in comparison to SiR-Actin.[26] Then bright and well resolved images were obtained with results similar to SiR-Actin (Fig. 5). The observed differences clearly result from different photophysical and physicochemical properties and (un)binding kinetics. In particular, in being absolutely neutral to F-actin polymerization rate, SITC-Actin may be beneficially exploited for undistorted F-actin monitoring in cell biology.

Conclusions

The new fluorescent labelling tool SITC is complementary to FITC, and shows balanced spectral properties as well as reasonable stability and good reactivity in organic solvents. *En route*, the newly developed synthesis allows gram-scale synthesis of the SiR and SITC fluorophores. In extending earlier reports,[37] we found that the triflate derived from phenol **10** is suitable for derivatisation and late stage diversification.

SITC can be used with readily available Cy5-compatible filters. It is an excellent label for fluorescence microscopy in living and fixed cells, as exemplified by high resolution imaging of F-Actin with SITC-Actin. SITC should hence become very useful for labelling of molecules, surfaces, and particles, or as a fluorophore partner in FRET applications. The unexpectedly high stability and attenuated reactivity of the SITC reagent in water (see ESI†) offers considerable potential for site-selective labelling reactions. Studies along this line are underway.

Conflicts of interest

There are no conflicts to declare.

Acknowledgements

Support by the DAAD (doctoral fellowship to V. N.) is gratefully acknowledged. Ms Jana Hamann (FLI Jena) is thanked for support in cell biology experimentation.

Notes and references

1 A. Baeyer, *Ber. Dtsch. Chem. Ges.*, 1871, **4**, 555–558.
2 Y. Urano, M. Kamiya, K. Kanda, T. Ueno, K. Hirose and T. Nagano, *J. Am. Chem. Soc.*, 2005, **127**, 4888–4894.
3 A. H. Coons, H. J. Creech and R. N. Jones, *Exp. Biol. Med.*, 1941, **47**, 200–202.
4 J. D. Marshall, W. C. Eveland and C. W. Smith, *Proc. Soc. Exp. Biol. Med.*, 1958, **98**, 898–900.
5 J. L. Riggs, R. J. Seiwald, J. H. Burckhalter, C. M. Downs and T. G. Metcalf, *Am. J. Pathol.*, 1958, **34**, 1081–1097.
6 G. T. Hermanson, *Bioconjugate Techniques*, 3rd edn, 2013, vol. 10, pp. 395–463.
7 M. Huang, Z. Ma, E. Khor and L. Y. Lim, *Pharm. Res.*, 2002, **19**, 1488–1494.
8 A. Imhof, M. Megens, J. J. Engelberts, D. T. N. de Lang, R. Sprik and W. L. Vos, *J. Phys. Chem. B*, 1999, **103**, 1408–1415.
9 M. Jullian, A. Hernandez, A. Maurras, K. Puget, M. Amblard, J. Martinez and G. Subra, *Tetrahedron Lett.*, 2009, **50**, 260–263.
10 T. C. Pappas, B. Gametchu and C. S. Watson, *FASEB J.*, 1995, **9**, 404–410.
11 Z. Qi, I. Whitt, A. Mehta, J. Jin, M. Zhao, R. C. Harris, A. B. Fogo and M. D. Breyer, *Am. J. Physiol.: Renal, Fluid Electrolyte Physiol.*, 2004, **286**, F590–F596.
12 S. Santra, H. Yang, D. Dutta, J. T. Stanley, P. H. Holloway, W. Tan, B. M. Moudgil and R. A. Mericle, *Chem. Commun.*, 2004, 2810–2811.
13 L. Ma, T. Dichwalkar, J. Y. H. Chang, B. Cossette, D. Garafola, A. Q. Zhang, M. Fichter, C. Wang, S. Liang, M. Silva, S. Kumari, N. K. Mehta, W. Abraham, N. Thai, N. Li, K. D. Wittrup and D. J. Irvine, *Science*, 2019, **365**, 162–168.
14 C. Song, J. Liu, J. Li and Q. Liu, *Biosens. Bioelectron.*, 2016, **85**, 734–739.
15 W.-L. Liu, S.-H. Lo, B. Singco, C.-C. Yang, H.-Y. Huang and C.-H. Lin, *J. Mater. Chem. B*, 2013, **1**, 928–932.
16 D. H. Ma, D. Kim, T. Akisawa, K. H. Lee, K. T. Kim and K. H. Ahn, *Chem. – Asian J.*, 2015, **10**, 894–902.
17 L. Wang, M. S. Frei, A. Salim and K. Johnsson, *J. Am. Chem. Soc.*, 2019, **141**, 2770–2781.
18 Y. Koide, Y. Urano, K. Hanaoka, T. Terai and T. Nagano, *ACS Chem. Biol.*, 2011, **6**, 600–608.
19 L. D. Lavis, *Annu. Rev. Biochem.*, 2017, **86**, 825–843.
20 L. D. Lavis and R. T. Raines, *ACS Chem. Biol.*, 2014, **9**, 855–866.
21 E. A. Specht, E. Braselmann and A. E. Palmer, *Annu. Rev. Plant Physiol.*, 2017, **79**, 93–117.
22 S. N. Uno, M. Kamiya, T. Yoshihara, K. Sugawara, K. Okabe, M. C. Tarhan, H. Fujita, T. Funatsu, Y. Okada, S. Tobita and Y. Urano, *Nat. Chem.*, 2014, **6**, 681–689.
23 K. Umezawa, M. Yoshida, M. Kamiya, T. Yamasoba and Y. Urano, *Nat. Chem.*, 2017, **9**, 279–286.
24 G. Lukinavicius, K. Umezawa, N. Olivier, A. Honigmann, G. Yang, T. Plass, V. Mueller, L. Reymond, I. R. Correa Jr.,

Z. G. Luo, C. Schultz, E. A. Lemke, P. Heppenstall, C. Eggeling, S. Manley and K. Johnsson, *Nat. Chem.*, 2013, **5**, 132–139.

25 G. Lukinavicius, G. Y. Mitronova, S. Schnorrenberg, A. N. Butkevich, H. Barthel, V. N. Belov and S. W. Hell, *Chem. Sci.*, 2018, **9**, 3324–3334.

26 G. Lukinavicius, L. Reymond, E. D'Este, A. Masharina, F. Gottfert, H. Ta, A. Güther, M. Fournier, S. Rizzo, H. Waldmann, C. Blaukopf, C. Sommer, D. W. Gerlich, H. D. Arndt, S. W. Hell and K. Johnsson, *Nat. Methods*, 2014, **11**, 731–733.

27 Y. Koide, Y. Urano, K. Hanaoka, W. Piao, M. Kusakabe, N. Saito, T. Terai, T. Okabe and T. Nagano, *J. Am. Chem. Soc.*, 2012, **134**, 5029–5031.

28 T. Wang, Q. J. Zhao, H. G. Hu, S. C. Yu, X. Liu, L. Liu and Q. Y. Wu, *Chem. Commun.*, 2012, **48**, 8781–8783.

29 B. Wang, X. Chai, W. Zhu, T. Wang and Q. Wu, *Chem. Commun.*, 2014, **50**, 14374–14377.

30 C. Fischer and C. Sparr, *Angew. Chem., Int. Ed.*, 2018, **57**, 2436–2440.

31 J. B. Grimm, T. A. Brown, A. N. Tkachuk and L. D. Lavis, *ACS Cent. Sci.*, 2017, **3**, 975–985.

32 K. Schwekendiek and F. Glorius, *Synthesis*, 2006, **18**, 2996–3002.

33 D. Göbel, N. Clamor and B. J. Nachtsheim, *Org. Biomol. Chem.*, 2018, **16**, 4071–4075.

34 C. J. Rohbogner, A. J. Wagner, G. C. Clososki and P. Knochel, *Org. Synth.*, 2009, **86**, 374–384.

35 S. van de Linde, A. Löschberger, T. Klein, M. Heidbreder, S. Wolter, M. Heilemann and M. Sauer, *Nat. Protoc.*, 2011, **6**, 991–1009.

36 R. Gerasimaite, J. Seikowski, J. Schimpfhauser, G. Kostiuk, T. Gilat, E. D'Este, S. Schnorrenberg and G. Lukinavicius, *Org. Biomol. Chem.*, 2020, **18**, 2929–2937.

37 E. Kozma, G. Estrada Girona, G. Paci, E. A. Lemke and P. Kele, *Chem. Commun.*, 2017, **53**, 6696–6699.

